Atomistic visualization of deformation in gold

Tokushi Kizuka
Department of Applied Physics, School of Engineering, Nagoya University, Furo-cho, Chikusa-ku, Nagoya 464-01, Japan and Research Center for Advanced Waste and Emission Management, Nagoya University, Furo-cho, Chikusa-ku, Nagoya 464-01, Japan
(Received 23 December 1997)

Atomistic visualization of deformation was realized by dynamic high-resolution transmission electron microscopy. Compression, tensile, and shear deformation in nanometer-sized gold was carried out at room temperature inside a 200-kV transmission electron microscope using a piezodriving specimen holder. The atomic process of the deformation was observed *in situ* at a spatial resolution of 0.2 nm and at a time resolution of $\frac{1}{60}$ s. It was shown that slip and twinning are attributed to the deformation and proceed at every atomic layer in dislocation-free nanometer-sized gold. A dislocationlike line defect is observed during the slip and twinning processes. [S0163-1829(98)04017-X]

INTRODUCTION

A mechanical force acting on a solid causes deformation and fracture. These two processes are closely related to several fields of technology and have been studied for a long time by scientists and engineers. In particular, the elucidation of the deformation process and its mechanism has been a fundamental subject in solid-state physics and metallurgy. Various types of deformation mechanisms have been proposed from mechanical tests and structure analyses, for example, dislocation mechanisms,[1–3] twinning,[4–6] and grain boundary sliding.[7,8] All of these mechanisms have been explained using atomistic models. According to these models, deformation proceeds through generation, multiplication, growth, and annihilation of line- and plane-type internal lattice defects, such as dislocations, stacking faults, and twins. Detailed studies have been performed for the elucidation of the relations between the deformation processes and the mechanisms. Several types of transmission electron microscopy (TEM) have played a significant role in this elucidation. For example, the structures of dislocations were investigated by conventional static TEM (Ref. 9) and it is known that their behaviors can be analyzed by conventional dynamic TEM using cinema photography.[10,11] In particular, the behaviors were directly observed by *in situ* deformation and conventional dynamic TEM.[12,13] The electron-irradiated-induced motions of twins in gold thin films[14] and gold clusters,[15] and surfaces and stacking faults in cadmium telluride[16,17] were also observed at an atomic level by dynamic high-resolution TEM (DHRTEM) using television camera and video tape recording systems. The deformation process, however, has not been directly observed in real space on an atomic scale and the elemental atomic processes in deformation have still not been clarified. A different type of microscopy is required in order to investigate the atomic processes: DHRTEM using a television camera and video tape recording system with a piezodriving specimen holder is expected to be the optimum method to analyze the atomic process of deformation.[18,19] The purpose of the present study is to elucidate the atomic processes of mechanical deformation in gold by direct atomistic visualization by DHRTEM.

EXPERIMENTAL PROCEDURES

A piezodriving specimen holder for a transmission electron microscope was developed for subnanometer scale mechanical deformation and *in situ* observations. Figure 1 is an illustration of the specimen holder. The mobile side is connected with a pipe-type piezoelectric device for fine displacement and a microscrew motor for coarse displacement. The specimen on the mobile side is mounted on the tip of a lever connected with the piezodevice. The mobile side are displaced along the x direction from 0 to 1 mm by the motor. The fine displacement along the x direction is controlled by homogeneous elongation and shrinkage of the piezodevice. The fine displacements along the y and z directions are controlled by elongation and shrinkage on one side of the pipe. Resolution of the fine displacement by the piezodevice is less than 0.16 nm along the x direction and 0.22 nm along the y

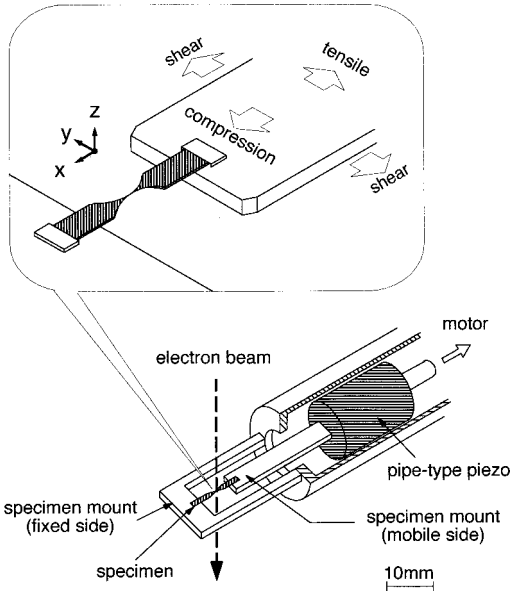

FIG. 1. Illustration of a piezodriving specimen holder for transmission electron microscopy for subnanometer-scale mechanical tests and *in situ* observations.

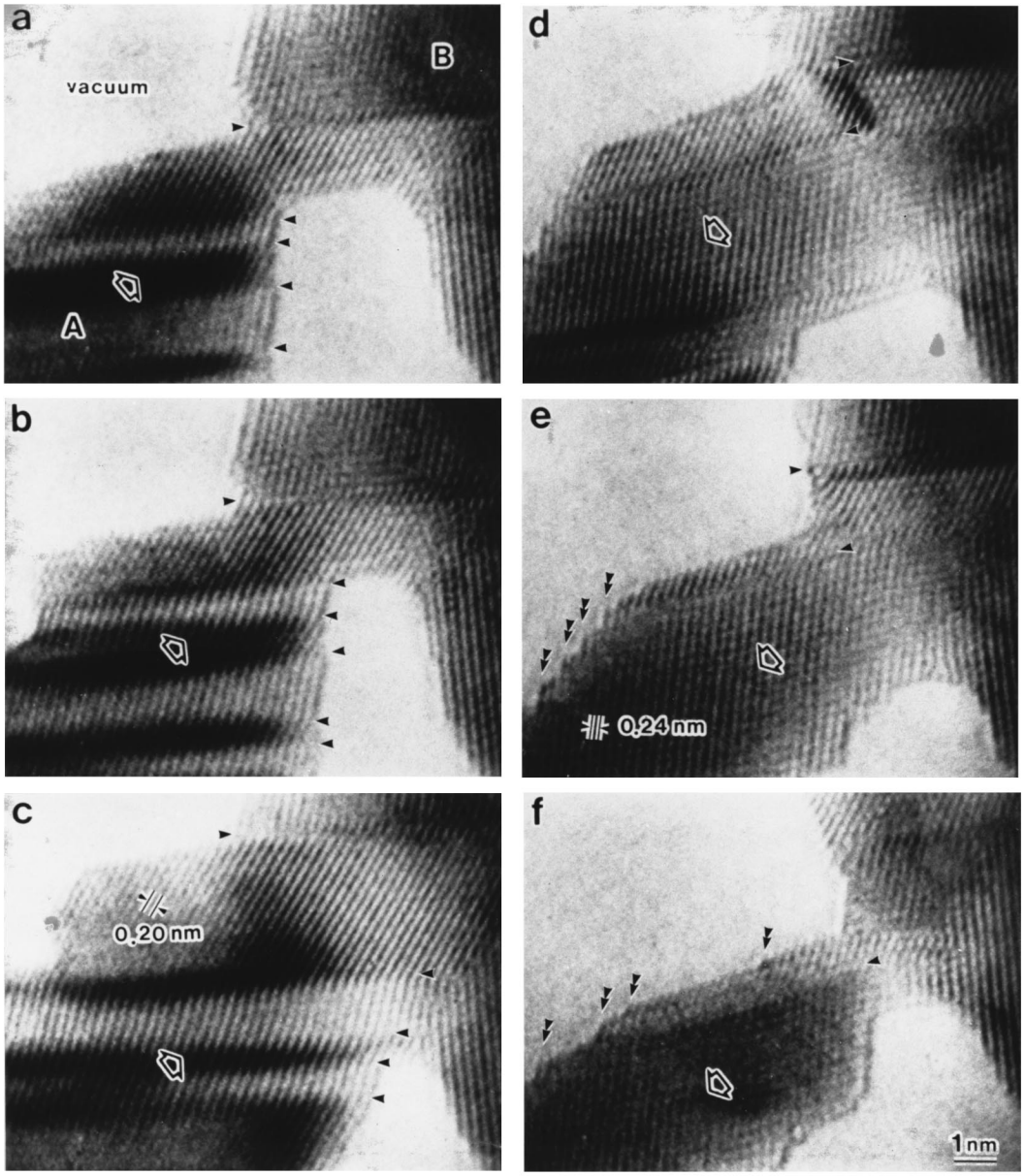

FIG. 2. Time-sequence series of high-resolution images of the process of compressing and tensile deformation in nanometer-sized gold. The specimen is connected with the mobile (A) and fixed (B) sides of the specimen holder. Bold arrows show the direction of displacement of the mobile side. Triangles show {111}/{111} $\Sigma=3$ twin boundaries. Double triangles show atomic-scale slip steps. The time in each image is (a) 0 s, (b) 4 s, (c) 11 s, (d) 16 s, (e) 23 s, and (f) 39 s.

and z directions. Piezodriving methods are used for the displacement of scanning needles in several combination-type microscopes of reflection electron microscopy and scanning tunneling microscopy (STM), or TEM and STM.[20–23]

The specimens used in the present work were gold wires, 0.1 mm in diameter. The tips of the wires were milled to nanometer size by Ar ions accelerated at 3 kV. Two needle-shaped specimens were separately placed at the fixed and mobile sides. The specimen holder was installed in a 200-kV high-resolution transmission electron microscope (JEOL, Ltd., JEM-2010). The two tips were bonded by controlling the piezodevice in the microscope at ambient temperature. The specimens for the subnanometer-scale mechanical deformation study were produced by the direct bonding as already reported elsewhere.[19] Structural variations in atomic arrangements were observed *in situ* using a silicon-integrated-target (SIT) television camera and a digital video tape recorder. In the image recording system, different images are obtained every field, i.e., a time resolution of the system is $\frac{1}{60}$ s.[18,19] The lattice resolution during the high-resolution observation using the present specimen holder was 0.14 nm.

RESULTS AND DISCUSSION

Figure 2 shows a time-sequence series of high-resolution images of the process of compressing and tensile deformation in the nanometer-sized gold. Each side of the specimen is connected to the mobile side (Fig. 2, A) and fixed (Fig. 2, B) side in the specimen holder. A grain boundary about 2.4 nm wide is observed in the center of Fig. 2(a). The {111} and

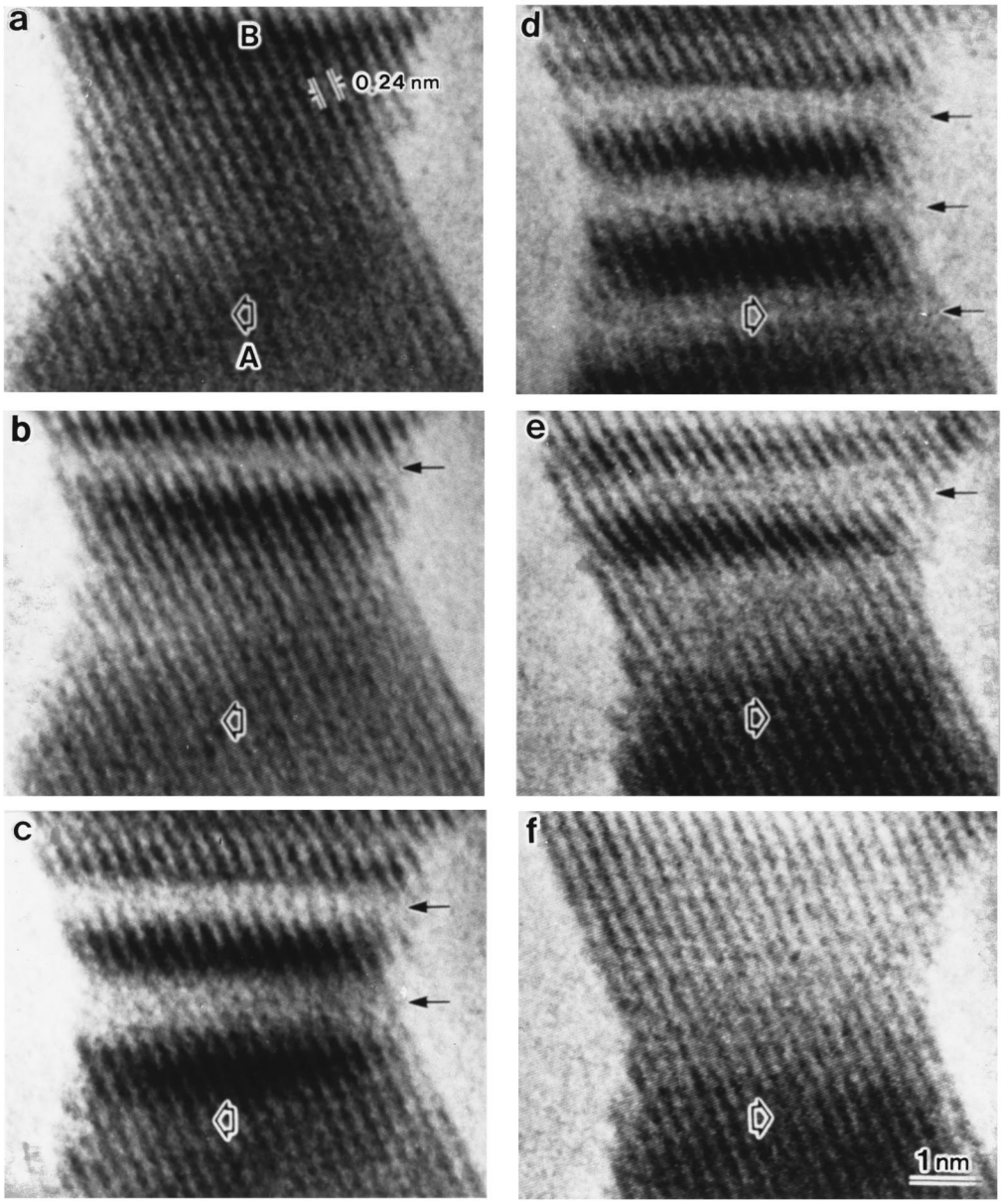

FIG. 3. Time-sequence series of high-resolution images of the process of shear tests in nanometer-sized gold. The specimen is connected with the mobile (A) and fixed (B) sides of the specimen holder. Bold arrows show the direction of displacement of the mobile side. Arrows show twinning. The time in each image is (a) 0/60 s, (b) 21/60 s, (c) 60/60 s, (d) 85/60 s, (e) 363/60 s, and (f) 387/60 s.

{200} lattice fringes of gold (lattice spacings $d_{111}=0.24$ nm and $d_{200}=0.20$ nm) clearly appear in all areas of the tips during the deformation. {111}/{111} $\Sigma=3$ twin boundaries are observed as shown by the triangles. The bright bands between the dark bands are twins. The tip on the mobile side is displaced along the direction indicated by open bold arrows. The average displacement speed is less than 0.1 nm/s. The specimen is deformed by the compressing force in Figs. 2(a)–2(c) and the tensile force in Figs. 2(c)–2(f). The twin boundaries generate, migrate, and annihilate during the process. Slip steps on an atomic scale form at the edges as shown by the double triangles [Figs. 2(e) and 2(f)] even when the behavior of the twin boundaries is not observed. This shows that slip is also attributed to the deformation. Similar deformation behavior appears when the displacement speed decreases.

Figure 3 shows a time-sequence series of high-resolution images of the shear deformation process in nanometer-sized gold. No grain boundary is observed around a contact boundary at the center during the initial state [Fig. 3(a)]. This is because the misorientation angle between the two tips before the contact is less than a few degrees and is accommodated by the rotation of the tips. A single-crystalline region is then prepared by the contact. A plane-type defect, such as a stacking fault or a twin boundary, is also not introduced in the region. The edge of the specimen on the mobile side (A) is displaced to the left-hand side in Figs. 3(a)–3(c) and to the right-hand side in Figs. 3(d)–3(f), as shown by the bold arrows. The displacement speed is less than 0.6 nm/s. First, twinning occurs in the upper part, as indicated by the arrow in Fig. 3(b). Subsequent twinning occurs in the middle [Fig. 3(c)] and the lower parts [Fig. 3(d)] when the tip on the

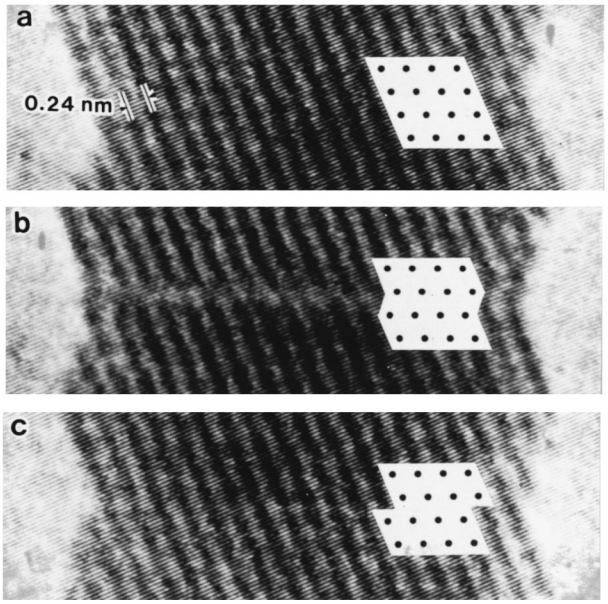

FIG. 4. Time-sequence series of high-resolution images of elemental processes of slip during the shear deformation in Fig. 3. An atomic arrangement projected along the [110] axis is inserted. The time in each image is (a) 0/60 s, (b) 86/60 s, and (c) 92/60 s.

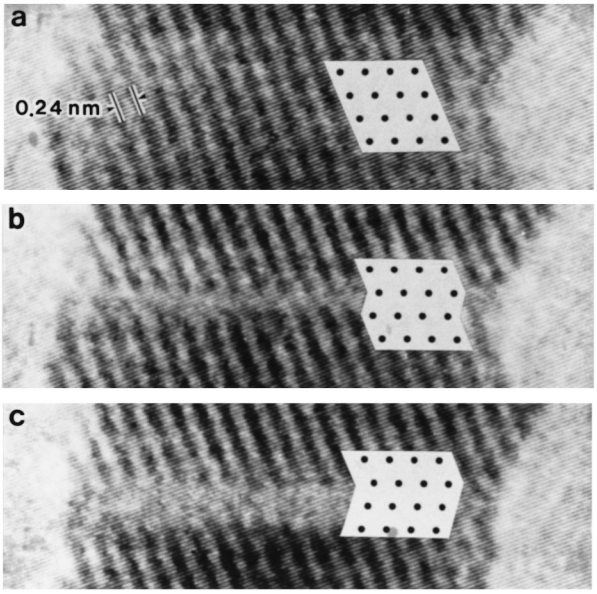

FIG. 5. Time-sequence series of high-resolution images of elemental processes of twinning during the shear deformation shown in Fig. 3. The atomic arrangement projected along the [110] axis is inserted. The time in each image is (a) 0/60 s, (b) 89/60 s, and (c) 91/60 s.

mobile side is displaced to the left side. The twinning then gradually recovers by the displacement of the tip to the right-hand side. Finally, the tips become a different single-crystalline structure. The deformation is thus a reversible one. The external shape of the specimen in the initial state, however, differs from that during the final state. This shows that slip is also attributed to the deformation, as shown in the next paragraph.

Figures 4 and 5 show time-sequence series of high-resolution images of the elemental atomic processes of slip and twinning during the shear deformation in Fig. 3, respectively. Figure 6 illustrates atomic arrangements of the process in Figs. 4 and 5. The atomic arrangements projected along the [110] and $[\bar{1}1\bar{1}]$ axes are shown on the left- and right-hand sides in each frame, respectively. First, stacking

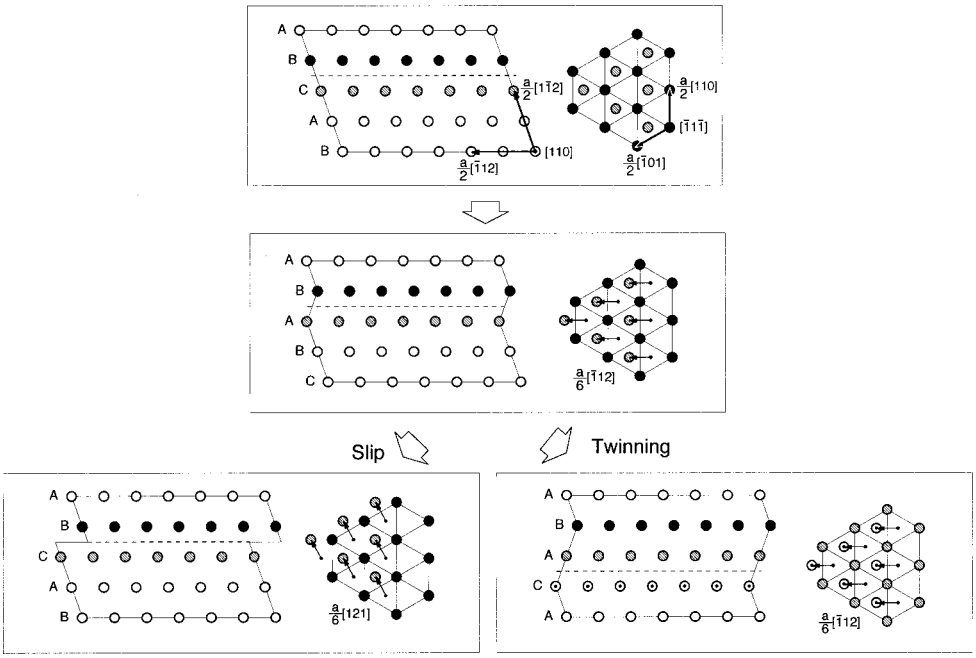

FIG. 6. Illustration of atomic arrangements projected along the [110] and $[\bar{1}1\bar{1}]$ axes in the process shown in Figs. 4 and 5. The atomic arrangement on the two atomic planes above and below the dotted line in the [110] projections is shown in the $[\bar{1}1\bar{1}]$ projections. The lattice constant of gold a is 0.41 nm.

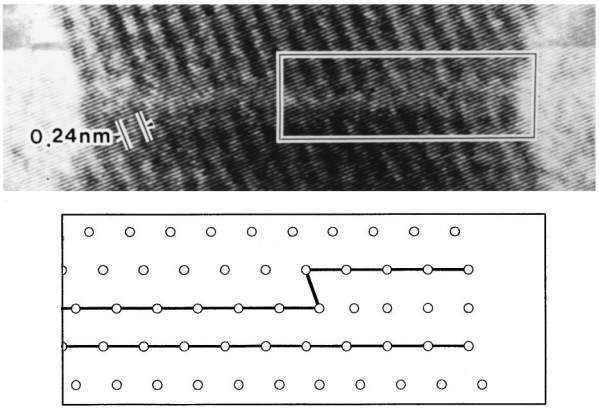

FIG. 7. Typical high-resolution image and its illustration of atomic arrangement of a dislocationlike line defect introduced during the displacement by $a/6[\bar{1}12]$ in the slip and twinning processes.

of atomic planes along the $[\bar{1}\bar{1}1]$ direction is *ABCAB* [Figs. 4(a) and 5(a)]. The lower part under the broken line as shown in Fig. 6 is displaced relative to the upper part by $a/6[\bar{1}12]$ due to mechanical force, where a is the lattice constant of gold. A stacking fault forms as shown in Figs. 4(b) and 5(b). The stacking sequence changes to *ABABC*. Slip then occurs when the lower part is displaced by $a/6[121]$ on the same plane. The stacking sequence becomes *ABCAB* again [Fig. 4(c)]. In the slip process, the lower part is displaced relatively to the upper part by $a/6[\bar{1}12]+a/6[121]=a/2[011]$. On the other hand, twinning takes place when the lower part is displaced by $a/6[\bar{1}12]$ on the (111) plane, which is lower by one (111) atomic plane of the previous stacking fault [Fig. 5(c)]. The lower part is displaced relatively to the upper part by $a/6[\bar{1}12]+a/6[\bar{1}12]=a/3[\bar{1}12]$ during the twinning process. The stacking becomes *ABACA*. These observations show that both slip and twinning occur and proceed on every atomic plane.

Figure 7 shows a typical high-resolution image and the atomic arrangement of an intermediate structure observed during the displacement by $a/6[\bar{1}12]$. Such structures appear in both the slip and twinning processes. These structures are observed only in one field image; they disappear within $\frac{2}{60}$ s or less. The positions of the atoms in the same (111) slip or twinning atomic plane change in the internal region; there is a dislocation-like localized line-type strained structure along the $[110]$ axis. The line-type strained structure is similar to that of a kind of partial dislocation with a Burgers vector equal to $a/6[\bar{1}12]$.

It is shown from the present observations that deformation proceeds by slip and twinning in the dislocation-free gold. It is well known that deformation of micrometer- or larger-sized gold at room temperature occurs by only slip due to multiplication and motion of dislocations.[1–3] Twinning in fcc metals takes place at low temperature and/or at a large deformation speed.[4–6,24–26] In the present study, deformation is carried out at room temperature and at a displacement speed of less than 0.6 nm/s. The present deformation condition does not correspond to the well-known twinning conditions. It is also reported that perfect dislocations with the Burgers vector equal to $a/2\langle 110\rangle$ or partial dislocations with the Burgers vector equal to $a/6\langle 211\rangle$ move easily on $\{111\}$ planes under the applied force along the $[211]$ direction.[1–3] We should point out other deformation conditions for the twinning; no dislocation is observed in the present specimens before the deformation. The critical shear stress for the twining will be similar to that for the slip in dislocation-free gold.

CONCLUSION

It was shown that atomic processes during the deformation in gold are directly visualized by DHRTEM. Contact, bonding, and separation processes between gold tips are observed using the same method as reported in our previous papers.[18,19] Various types of mechanical tests can be performed on an atomic scale by the present specimen piezodriving method for the investigation of behaviors of atomic-scale contact boundaries, such as formation of atomic bridges and electric conductance quantization.[27–31] A different type of study concerning the mechanical properties of crystals has been opened on an atomic scale.

ACKNOWLEDGMENTS

The author would like to thank the late Professor Yoichi Ishida of Tokyo University, Professor Hiroshi Fujita of Osaka University, and Professor Shigeo Okuda of Tsukuba University for their helpful discussions. The author also wishes to thank Katsuyoshi Kumazawa of the Department of Applied Physics Work Shop of Nagoya University for help with the production of the specimen preparation vacuum chamber, and S. Deguchi and M. Naruse of JEOL, Ltd. for help with the development of the piezodriving specimen holder. Financial support was provided by the Yazaki Memorial Foundation for Science and Technology, the Amada Foundation for Metal Works Technology, the Tatematsu Foundation, TEPCO Research Foundation, Kawasaki Steel 21st Century Foundation, and the Sumitomo Foundation. The present study was partly supported by a Grant-In-Aid from the Ministry of Education, Science and Culture, in Japan.

[1] A. H. Cottrell, *Theory of Crystal Dislocations* (Gordon and Breach, New York, 1964).
[2] J. P. Hirth and J. Lothe, *Theory of Dislocations* (McGraw-Hill, New York, 1968).
[3] F. R. N. Nabarro, *Crystal Dislocations* (Oxford Clarendon, New York, 1968).
[4] R. W. Cahn, Adv. Phys. **3**, 363 (1945).
[5] E. O. Hall, *Twinning and Diffusionless Transformation in Metals* (Buterworths, London, 1954).
[6] M. V. Klassen-Neklyyudova, *Mechanical Twinning of Crystals* (Consultants Bureau, New York, 1964).
[7] *Grain Boundary Structure and Properties*, edited by G. A. Chadwick and D. A. Smith (Academic, London, 1976).
[8] *Towards Innovation in Superplasticity*, edited by T. Sakuma, T.

Aizawa, and K. Higashi (Trans Tech, Uetikon-Zuerich, 1996).
[9] P. B. Hirsch, A. Howie, R. Nicholson, D. W. Pashley, and M. J. Whelan, *Electron Microscopy of Thin Crystals* (Krieger, Malabar, FL, 1977).
[10] P. B. Hirsch, R. W. Horne, and M. J. Whelan, Philos. Mag. **1**, 667 (1956).
[11] H. Hashimoto, K. Tanaka, K. Kobayashi, and S. Shimizu, *Proceedings of the Fourth International Conference on Electron Microscopy* (Springer, Berlin, 1958); H. Hashimoto, J. Electron Microsc. **9**, 130 (1960).
[12] H. Fujita and H. Yamada, Trans. Jpn Inst. Met. **9**, 943 (1968).
[13] H. Saka and T. J. Imura, J. Phys. Soc. Jpn. **32**, 702 (1972).
[14] H. Hashimoto, Y. Yokota, Y. Takai, H. Endoh, and A. Kumao, Chem. Scr. **14**, 125 (1978); H. Hashimoto, Y. Takai, Y. Yokota, H. Endoh, and E. Fukada, Jpn. J. Appl. Phys. **19**, L1 (1980).
[15] S. Iijima and T. Ichihashi, Phys. Rev. Lett. **56**, 616 (1986).
[16] R. Scinclair, T. Yamashita, and F. A. Ponce, Nature (London) **290**, 386 (1981).
[17] R. Scinclair, F. A. Ponce, T. Yamashita, D. A. Smith, R. A. Camps, L. A. Freeman, S. J. Erasmus, W. C. Nixon, K. C. A. Smith, and C. J. D. Catto, Nature (London) **298**, 127 (1982).
[18] T. Kizuka, K. Yamada, S. Deguchi, M. Naruse, and N. Tanaka, Phys. Rev. B **55**, R7398 (1997).
[19] T. Kizuka, K. Yamada, S. Deguchi, M. Naruse, and N. Tanaka, J. Electron Microsc. **2**, 151 (1997).
[20] M. Kuwabara, W. K. Lo, and J. C. H. Spence, J. Vac. Sci. Technol. A **7**, 2745 (1989).
[21] J. C. H. Spence, Ultramicroscopy **25**, 165 (1988).
[22] M. I. Lutwyche and Y. Wada, Appl. Phys. Lett. **66**, 2807 (1994).
[23] Y. Naitoh, K. Takayanagi, and M. Tomitori, Surf. Sci. **357-358**, 208 (1996).
[24] T. H. Blewitt, P. R. Coltman, and J. K. Redman, J. Appl. Phys. **28**, 651 (1957).
[25] P. Hassen, Philos. Mag. **3**, 384 (1958).
[26] C. S. Smith, Trans. Metall. Soc. AIME **214**, 574 (1958).
[27] T. N. Todorov and A. P. Sutton, Phys. Rev. Lett. **70**, 2138 (1993).
[28] A. M. Bratkovsky, A. P. Sutton, and T. N. Todorov, Phys. Rev. B **52**, 5036 (1995).
[29] L. Olesen, E. Lægsgaard, I. Stensgaard, F. Besenbacher, J. Schiøtz, P. Stoltze, K. W. Jacobsen, and J. K. Nørskov, Phys. Rev. Lett. **72**, 2252 (1994).
[30] J. M. Krans, J. M. van Ruitenbeek, V. V. Fisun, I. K. Yanson, and L. J. de Jongh, Nature (London) **375**, 767 (1995).
[31] K. Murooka, M. Mitome, Y. Tanishiro, and K. Takayanagi, J. Vac. Sci. Technol. A **8**, 153 (1990).